JOC The Journal of Organic Chemistry

Article

pubs.acs.org/joc

Computational and NMR Spectroscopic Evidence for Stereochemistry-Dependent Conformations of 2,2,6,6-Tetramethylpiperidinyl-Masked 1,2-Diols

Ellie L. Fought,[†] Shreyosree Chatterjee,[†] Theresa L. Windus,* and Jason S. Chen*

Department of Chemistry, Iowa State University, Ames, Iowa 50011, United States

Supporting Information

ABSTRACT: 2,2,6,6-Tetramethylpiperidinyl-masked 1,2-diols exhibited stereochemistry-dependent hydroxyl proton chemical shifts: ca. 7 ppm for the *syn* diastereomer and ca. 2 ppm for the *anti* diastereomer. A computational search for low energy geometries revealed that the *syn* isomer favors a six-membered ring hydrogen bond to nitrogen and the *anti* isomer favors a five-membered ring hydrogen bond to oxygen. The computed low energy conformations were found to have a large difference in hydroxyl proton shielding that was reflected in the experimental chemical shift difference. This chemical shift difference was observed in a broad range of solvents, and thus may be useful as a stereochemical probe. The stereochemistry-dependent conformation and chemical shift signature appeared to be due to a *syn* pentane interaction between the *gem*-dimethyl groups on the 2,2,6,6-tetramethylpiperidinyl moiety.

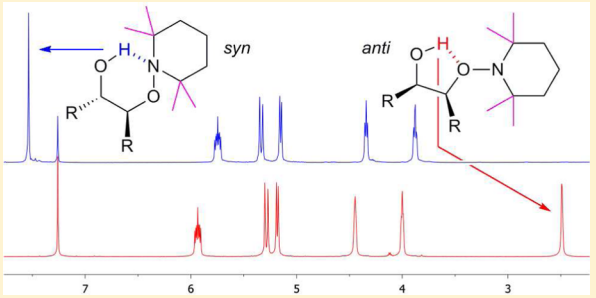

INTRODUCTION

Stereochemically defined polyols are commonly found in natural products and bioactive molecules. Oxidative strategies for introducing alcohols or masked alcohols are appealing because they install additional functional groups. Many oxidants have been used to introduce alcohols, including osmium tetroxide,[1] selenium dioxide,[2] singlet oxygen,[3] and oxaziridine reagents.[4] More recently, the readily available stable oxygen radical 2,2,6,6-tetramethyl-1-piperidinyloxy (TEMPO) has become increasingly popular as a precursor to an electrophilic oxygen reagent. TEMPO has been used to install 2,2,6,6-tetramethylpiperidinyl-masked alcohols through α-functionalization reactions of carbonyl compounds[5] and β-dicarbonyls[6] and vicinal difunctionalization reactions of alkenes[7] and α,β-unsaturated carbonyl compounds.[8]

We recently reported that α-oxyaldehydes generated by oxidative incorporation of TEMPO can react with diverse organomagnesium or organolithium reagents to yield differentially masked *anti*-1,2-diols, in many cases with a >20:1 diastereomeric ratio.[9] In the course of that study, we noticed that the NMR chemical shift of the hydroxyl proton in 2,2,6,6-tetramethylpiperidinyl-masked 1,2-diols is strongly dependent on the stereochemistry of the diol. (For clarity, throughout this paper, 2,2,6,6-tetramethylpiperidinyl-masked 1,2-diols are referred to simply as diols. There are no unprotected diols in this paper.) The hydroxyl chemical shift in $CDCl_3$ is ca. 6 ppm for primary alcohols **1** (Figure 1), ca. 7 ppm for *syn* diols **2**, and ca. 2 ppm for *anti* diols **3**. Herein, we provide computational and NMR spectroscopic evidence that this chemical shift anomaly reflects differences in the ground state conformations of such compounds.

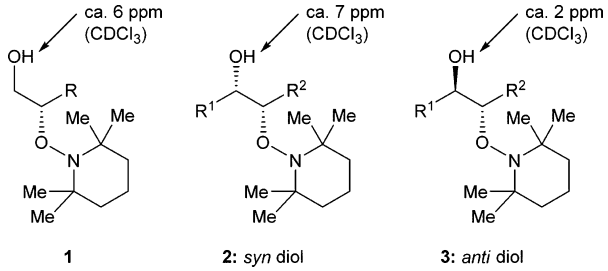

Figure 1. 2,2,6,6-Tetramethylpiperidinyl-masked diols.

Results and Discussion. The ^1H NMR spectra for differentially masked diols **1a** (R = *n*-propyl) and **2a** and **3a** (R^1 = vinyl, R^2 = *n*-propyl) are shown in Figure 2. Synthetic diols **2a** (*syn*) and **3a** (*anti*) were chosen for NMR spectroscopic studies because the ^1H NMR signals for the two hydrogens next to the oxygen-bound carbons could be unambiguously assigned since only one is allylic. Secure assignment of these two signals was critical for enabling coupling-constant-based conformational analysis.[10] The identity of the hydroxyl protons was confirmed by deuterium exchange with D_2O. Whereas hydroxyl protons in $CDCl_3$ typically display variable chemical shifts and often are absent due to their rapid exchange with protons from adventitious water, the hydroxyl protons in diols **1**–**3** had reproducible chemical shifts and did not undergo rapid proton exchange with water. The slow rate of proton exchange suggested the presence

Received: July 2, 2015
Published: October 1, 2015

DOI: 10.1021/acs.joc.5b01516
J. Org. Chem. 2015, 80, 9967–9972

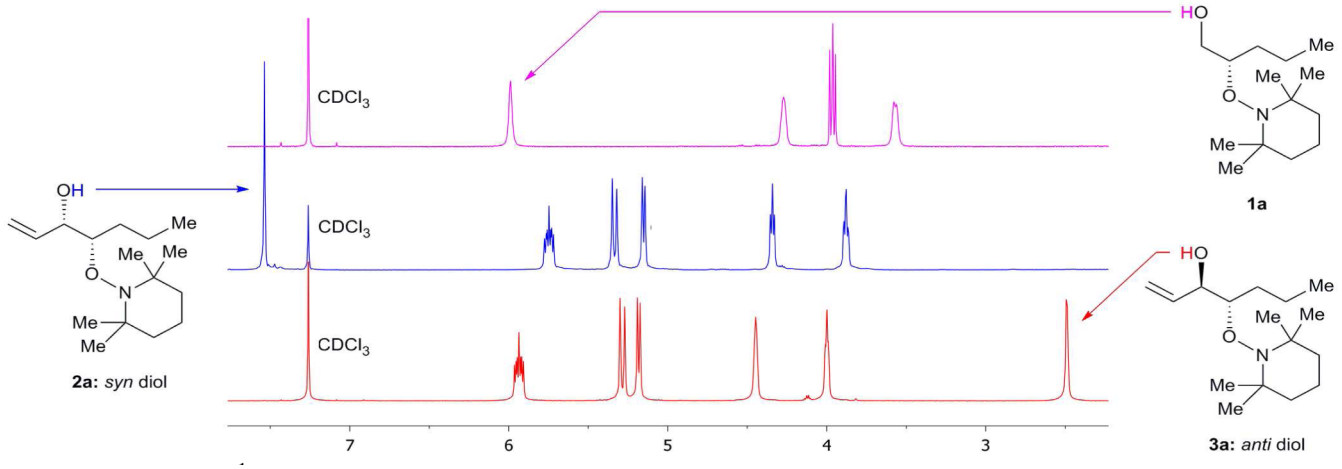

Figure 2. Partial ^{1}H NMR spectra of diols **1a**, **2a**, and **3a**. See the Supporting Information for full-width spectra.

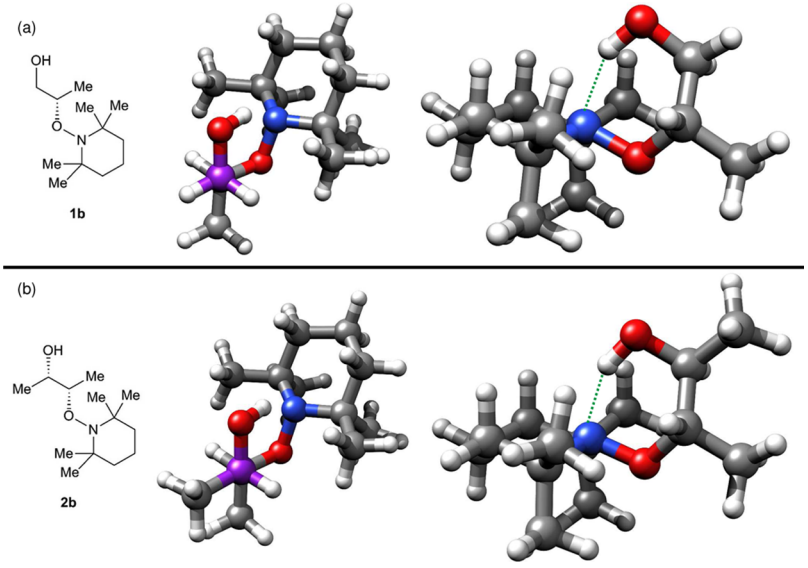

Figure 3. Computed ground state conformations of (a) primary diol **1b** and (b) *syn* diol **2b**. Two different views are given for each conformation. The purple atom is a carbon directly in front of another carbon in a Newman projection-like view.

of intramolecular hydrogen bonding. The hydroxyl proton could hydrogen bond to the oxygen of the masked alcohol to form a five-membered ring or to the nitrogen of the piperidine ring to form a six-membered ring. The large chemical shift differences between *syn* diols **2** and *anti* diols **3** suggested that these diastereomeric compounds may adopt different ground state conformations.

Since the unusual hydroxyl proton NMR chemical shifts were observed across all compounds of structures **1**−**3** that we have characterized thus far,[9] computational studies could be performed using the simplest possible carbon backbones. The computational analysis of primary alcohol **1b**, *syn* diol **2b**, and *anti* diol **3b** (all with R = R^1 = R^2 = Me) began with a systematic identification of the low energy conformations. Three to five of the lowest energy conformations were chosen for each compound as starting points for higher-level analysis. All structures shown in this paper are at the MP2/6-311G(d,p) level, and all energies include zero point energy (ZPE) corrections. The element colors in the figures are as follows: nitrogen is blue, oxygen is red, carbon is gray, and hydrogen is white.

After the final round of geometry optimizations, a low energy geometry emerged for each of the compounds (**1b**−**3b**). The structures shown in Figures 3 and 4 do not emphasize visualization of the piperidinyl ring, but in all cases, this ring possesses a chair conformation with the oxygen substituent in an equatorial position.

The computed geometry of primary alcohol **1b** (Figure 3a) shows an intramolecular hydrogen bond between the hydroxyl proton and the piperidine nitrogen (1.85 Å). The six-membered ring formed by hydrogen bonding adopts a twist boat conformation, and the alkyl chain of the diol backbone is *anti* to the free hydroxyl group. While the lowest energy conformation contains a six-membered ring hydrogen bond, the lowest energy conformation with a five-membered ring hydrogen bond is only 3.3 kcal mol^{-1} higher in energy (see Table 1). The Boltzmann ratios between the different five- and six-membered rings are also given to show the populations of the different conformations at room temperature.

The computed geometry of *syn* diol **2b** (Figure 3b) is virtually identical to that of primary alcohol **1b** (1.85 Å hydrogen bond for **1b**; 1.81 Å for **2b**), save for the presence of

DOI: 10.1021/acs.joc.5b01516
J. Org. Chem. 2015, 80, 9967−9972

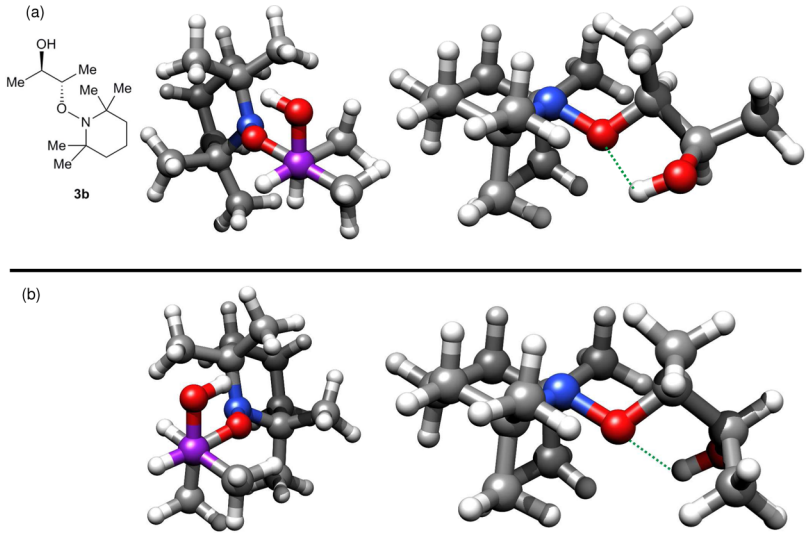

Figure 4. Computed geometries for (a) the lowest energy conformation of *anti* diol **3b** and (b) the second-lowest energy conformation of diol **3b**. Two different views are given for each conformation. The purple atom is a carbon directly in front of another carbon in a Newman projection-like view.

Table 1. Relative Energy and Boltzmann Populations of Five- and Six-Membered Ring Hydrogen Bond Conformations

compound	ΔE/kcal mol^{-1}[a]	Boltzmann population ratios at 298 K[b]
1b	+3.3	99.6:0.4
2b	+3.4	99.7:0.3
3b	−2.7	0.9:80.3:18.8[c]
1b′	+1.2	88.5:11.5
2b′	+0.9	82.0:18.0
3b′	+0.6	57.5:42.5

[a]The energy difference is calculated for the lowest energy five- and six-membered ring hydrogen bond conformations. A positive energy indicates that the six-membered ring hydrogen bond conformation is lower in energy. [b]Calculated ratio of six-membered ring hydrogen bond conformation to five-membered ring hydrogen bond conformation at room temperature. [c]Ratio of the six-membered ring hydrogen bond conformation to the lowest and next-lowest energy five-membered ring hydrogen bond conformation at room temperature.

an additional alkyl group *anti* to the masked hydroxyl group. The *anti* relationship between the two methine protons (and thus the gauche relationship of the diol alkyl groups) was experimentally validated by the observation of a large $^3J_{H-H}$ coupling constant (8.7 Hz) between these two protons in the ^{1}H NMR spectrum of *syn* diol **2a**.[10] The lowest energy five-membered ring hydrogen bond conformation is 3.4 kcal mol^{-1} higher in energy than the lowest six-membered ring structure.

As shown in Figure 4, the two lowest energy computed geometries of *anti* diol **3b** possess a five-membered ring hydrogen bond between the hydroxyl proton and the oxygen of the masked hydroxyl. The two five-membered ring geometries were calculated to have similar energies (separated by only 0.9 kcal mol^{-1}) and hydrogen bond distances (2.21 Å for the lower energy geometry; 2.25 Å for the higher energy geometry). This hydrogen bond length is significantly longer than those for **1b** and **2b** and is likely due to the need to minimize torsional strain in the five-membered ring. A transition state between these two geometries was located computationally at 6.3 kcal mol^{-1} above the lower energy geometry, suggesting that these two structures

Table 2. Computed and Experimental Hydroxyl Proton Chemical Shifts

solvent	primary alcohol/ppm	*syn* diol/ppm	*anti* diol/ppm
gas phase (computed)	5.51 (**1b**)[a]	6.98 (**2b**)[a]	0.00 (**3b**)[b]
			2.05 (**3b**)[a,c]
$CDCl_3$	5.99 (**1a**)	7.55 (**2a**)	2.49 (**3a**)
benzene-d_6	5.40 (**1a**)	7.16 (**2a**)[d]	1.87 (**3a**)
cyclohexane-d_{12}	4.68 (**1a**)	6.49 (**2a**)	1.75 (**3a**)
CD_3CN	5.94 (**1a**)	6.66 (**2a**)	2.71 (**3a**)
THF-d_8	4.44 (**1a**)	6.36 (**2a**)	3.54 (**3a**)
acetone-d_6	4.75 (**1a**)	6.93 (**2a**)	3.46 (**3a**)
DMF-d_7	4.58 (**1a**)	6.00 (**2a**)	4.50 (**3a**)
DMSO-d_6	4.59 (**1a**)	6.42 (**2a**)	4.51 (**3a**)
pyridine-d_5	5.94 (**1a**)	7.17 (**2a**)	6.06 (**3a**)
CD_3OH:$CDCl_3$ (1:1)	5.51 (**1a**)	6.98 (**2a**)	[e]

[a]Referenced to the calculated isotropic chemical shift of the lower energy conformation of diol **3b**. [b]The calculated isotropic chemical shift for the lower energy conformation of diol **3b** was set to 0.00 ppm. [c]Calculated for the higher energy conformation of diol **3b**. [d]Hydroxyl proton signal is hidden under the solvent residual peak. Blending in a small amount of $CDCl_3$ shifts the hydroxyl proton signal downfield. [e]Hydroxyl proton signal is either hidden under the CD_3OH hydroxyl proton signal or rapidly exchanging with the CD_3OH hydroxyl proton signal.

DOI: 10.1021/acs.joc.5b01516
J. Org. Chem. 2015, 80, 9967−9972

rapidly equilibrate at ambient temperature. The hydrogen bond to oxygen shortens in the transition state to 1.87 Å. HETLOC NMR spectroscopy of *anti* diol **3a** revealed a 4 Hz $^{3}J_{H-H}$ coupling constant between the methine protons, consistent with a gauche relationship between these two protons (and thus a gauche relationship between the diol alkyl groups). Measurement of $^{2}J_{C-H}$ and $^{3}J_{C-H}$ coupling constants by HETLOC and PS-HMBC NMR spectroscopy, respectively,[10] did not allow unambiguous identification of the major conformation, but 1D NOE data provided evidence for the presence of both conformations shown in Figure 4. The lowest energy six-membered ring hydrogen bond conformation is 2.7 kcal mol^{-1} higher in energy than the lowest energy five-membered ring.

Isotropic chemical shifts were calculated for the lowest energy conformations of diols **1b**−**3b** (see Table 2). The KT2 functional[11] was favored over B3LYP[12] because KT2 was designed specifically for the calculation of magnetic properties. The computed hydroxyl proton chemical shifts for diols **1b**−**3b** are in good qualitative agreement with the experimental chemical shifts for diols **1a**−**3a** in $CDCl_3$. Interestingly, even though the computed low energy geometries of diols **1b** and **2b** are very similar, the computed hydroxyl proton chemical shifts nonetheless correctly reflect not only the experimentally observed relative shielding of the hydroxyl protons but also even the magnitude of the difference. This close agreement provides strong evidence that the computed gas phase conformations of diols **1b**−**3b** are relevant in solution.

Similar differences in shielding between the hydroxyl protons of diols **1a**−**3a** are observed in other solvents with weak Lewis basicity, suggesting that the calculated conformational preferences are retained. The chemical shift of the hydroxyl protons of primary alcohol **1a** and *syn* diol **2a** are little affected by solvents with stronger Lewis basicity, but the hydroxyl proton of *anti* diol **3a** shifts downfield. This change might be due to a competition between intramolecular hydrogen bonding and hydrogen bonding to the more Lewis basic solvents; alternatively, these solvents might reduce the energy gap between the five- and the six-membered ring intramolecular hydrogen bond conformations. Nonetheless, the relative shielding as compared with *syn* diol **2a** is preserved, and thus, this chemical shift difference is a useful stereochemical probe across a broad range of solvents. Interestingly, despite the ability to compensate for loss of an intramolecular hydrogen bond by hydrogen bonding to CD_3OH, the proton exchange for diols **1a** and **2a** is sufficiently slow that their characteristic hydroxyl proton chemical shifts can be observed even in a 1:1 CD_3OH:$CDCl_3$ mixture. ($CDCl_3$ was added in order to improve solubility.) Therefore, the six-membered ring hydrogen bond conformation of primary alcohol **1a** and *syn* diol **2a** appears to be surprisingly stable even in protic solvent.

To try to understand why diastereomeric diols **2** and **3** favor different conformations, we investigated the role of the *gem*-dimethyl groups on the 2,2,6,6-tetramethylpiperidinyl moiety by computing the low energy geometries for diols **1′**−**3′** (Figure 5). In all cases, a six-membered ring hydrogen bond conformation is favored, but the energy difference between five- and six-membered ring hydrogen bond conformations is smaller than the corresponding energy difference for diols **1b**−**3b** (see Table 1). The *syn* pentane interaction between the axial methyl groups on the piperidine ring of diols **1**−**3** forces these methyl groups apart (N−C−C_{axial} angles for **1b**: 115.0° and 115.3°; N−C−H_{axial} angles for **1′**: 109.6° and 109.9°; all

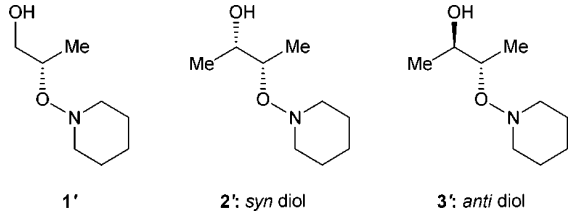

Figure 5. Diols masked by unmethylated piperidinyl moieties.

angles measured on the lowest energy conformation) and flattens the chair conformation at nitrogen (C−N−C angle for **1b**: 117.2°; for **1′**: 110.9°). Similar angles are observed for all five- and six-membered ring conformations of diols **1b**−**3b** and for diols **1′**−**3′**. This *syn* pentane-induced distortion does not consistently favor a five- or six-membered ring hydrogen bond conformation, but nonetheless appears to be causing diols **1**−**3** to have distinct preferred conformations and NMR spectroscopic signatures.

CONCLUSION

The stereochemistry-dependent hydroxyl proton chemical shift of 2,2,6,6-tetramethylpiperidinyl-masked 1,2-diols was shown by a combination of computational and NMR spectroscopic methods to be the result of differences in ground state conformations. Primary alcohols **1** and *syn* diols **2** favor a six-membered ring hydrogen bond, but *anti* diols **3** favor a five-membered ring hydrogen bond. Computed isotropic chemical shifts of the hydroxyl protons show good correlation with experimental chemical shifts. The hydroxyl proton of *syn* diols **2** is downfield of the hydroxyl proton of *anti* diols **3** in a broad range of solvents, making this difference in chemical shift useful for assigning relative stereochemistry. These stereochemistry-dependent conformational and spectroscopic differences appear to stem from a *syn* pentane interaction on the tetramethylpiperidine ring.

The internal hydrogen bonding forces the carbon chain of the diol to adopt a gauche conformation in both *syn* diols **2** and *anti* diols **3**. This bending of the carbon chain is expected to enhance ring closure rates of substrates containing a 2,2,6,6-tetramethylpiperidinyl-masked 1,2-diol. Furthermore, the predictable direction of the bend for *syn* diols **2** may be useful for remote stereoinduction in cyclization reactions. Studies to explore these potential synthetic consequences of the conformational preferences discovered herein are under way.

EXPERIMENTAL SECTION

Computation. The General Atomic and Molecular Electronic Structure System (GAMESS) software package[13] was used for all structure analysis calculations. The systematic identification of low energy conformations was performed using Restricted Hartree−Fock (RHF) and the small basis set 3-21G(d).[14] The optimization process began by finding a stable, low energy conformation for the tetramethylpiperidine ring by twisting the ring in the known conformations (boat, chair, twisted chair, for example). A systematic rotor search around all of the rotatable chain bonds then followed for each diol's required stereochemistry. Between 15 and 20 different conformations of each compound were found in the optimization process. All equilibrium coordinates are provided in the Supporting Information. The lowest energy geometries within a 4 kcal/mol window (three to five geometries) were used in higher-level calculations. Further optimizations were performed using both B3LYP[12] density functional theory and Møller−Plesset second-order perturbation theory (MP2)[15] using the 6-311G(d,p) basis set.[16] Since the B3LYP and MP2 geometries were very similar, Hessians were only

DOI: 10.1021/acs.joc.5b01516
J. Org. Chem. 2015, 80, 9967−9972

computed at the B3LYP/6-311G(d,p) level to confirm that minima were found and to obtain the zero point energy (ZPE) corrections. The images in the paper were generated using Chimera.[17]

Chemical shielding calculations were performed using the NWChem computational software package with a fine grid and a wave function DIIS error vector of less of 1.0×10^{-5}.[18] The Gauge-Independent Atomic Orbital (GIAO) method[19] was employed with the KT2 functional[11] and the aug-cc-pVTZ basis set[20] using the MP2/6-311G(d,p) optimized geometries. Shielding tensors of the B3LYP optimized structures for each compound were calculated, and the isotropic shielding values were then used to calculate the chemical shifts. For completeness, shielding calculations for the lowest energy structures were also performed using the B3LYP functional. The results using B3LYP provided the same trend in chemical shifts and are available in the Supporting Information. In this paper, only the shifts for the lowest energy structure for each compound are reported in the text and the others are available in the Supporting Information. The higher energy compounds have the same trends as those for the lowest energy conformations with respect to the different compounds and the formation of a five- or six-membered ring.

Synthesis. See Scheme 1. All reactions were performed with stirring under an argon atmosphere under anhydrous conditions.

Scheme 1. Synthesis of Diols 1a−3a

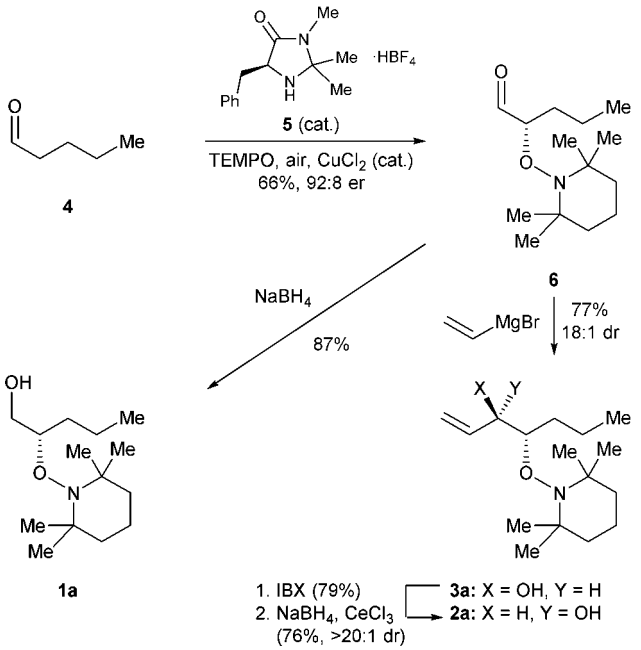

Vinylmagnesium bromide solution was purchased from Aldrich. All other reagents were purchased at the most economical grade. Dry tetrahydrofuran (THF) was obtained by passing HPLC grade solvent through a commercial solvent purification system. All other chemicals were used as received, without purification. Flash column chromatography was performed using Grace Davison Davisil silica gel (60 Å, 35−70 μm). Yields refer to chromatographically and spectroscopically (^{1}H NMR) homogeneous samples of single diastereomers. Thin-layer chromatography (TLC) was performed on Grace Davison Davisil silica TLC plates using UV light and common stains for visualization. NMR spectra were calibrated using residual undeuterated solvent as an internal reference. Apparent couplings were determined for multiplets that could be deconvoluted visually.

α-Oxyaldehyde ***6*** *((S)-2-((2,2,6,6-Tetramethylpiperidin-1-yl)oxy)-pentanal).* To a mixture of activated 4 Å molecular sieves (100 mg, powdered) and imidazolidinone catalyst **5** ((*S*)-5-benzyl-2,2,3-trimethylimidazolidin-4-one) (500 mg, 1.6 mmol, 0.2 equiv) in 5 mL of acetone was added $CuCl_2 \cdot 2H_2O$ (139 mg, 0.81 mmol, 0.1 equiv). The green reaction mixture was stirred open to air for 5 min until the copper salt dissolved and the mixture turned dark orange. The reaction was cooled to 0 °C for 10 min; then, pentanal (**4**, 0.87 mL, 8.1 mmol, 1.0 equiv) was added dropwise over 2 min. The reaction was stirred at 0 °C for 10 min; then, a solution of TEMPO (1.51 g, 9.7 mmol, 1.2 equiv) in 2 mL of acetone was added dropwise over 3 min. The reaction mixture was capped with a rubber septum, and an air inlet line was attached via an 18-gauge needle. The reaction was stirred at 0 °C for 24 h, then partitioned between ether (15 mL) and saturated NH_4Cl (45 mL). The aqueous layer was extracted with ether (2 × 45 mL), and the combined organic layers were washed with brine (90 mL). The organic layer was dried over Na_2SO_4, filtered, and concentrated to give an orange oil. Flash column chromatography (5% EtOAc/hexanes) gave α-oxyaldehyde **6** (1.30 g, 66% yield) as a colorless oil. A sample was derivatized [1. $NaBH_4$, MeOH; 2. *m*-nitrobenzoyl chloride, Et_3N, DMAP (cat.), CH_2Cl_2; 3. Zn, AcOH, THF, H_2O] and determined by chiral HPLC [Chiraltech IC column, 2.1 × 100 mm, 3 μm; 10% *i*-PrOH/hexanes, 0.2 mL/min, 25 °C; 280 nm UV detection; R_t = 8.8 (major), 9.9 (minor) minutes] to have 92:8 er. **6:** R_f = 0.47 (5% EtOAc/hexanes); $[\alpha]_D^{23} = -90.5°$ (*c* = 1.00, $CHCl_3$); IR (thin film): ν_{max} = 2933, 1732 cm^{-1}; ^{1}H NMR (600 MHz, $CDCl_3$): δ = 9.77 (d, *J* = 4.5 Hz, 1H), 4.08 (m, 1H), 1.70 (m, 1H), 1.64 (m, 1H), 1.50−1.08 (m, 20H), 0.92 (t, *J* = 7.4 Hz, 3H) ppm; ^{13}C NMR (150 MHz, $CDCl_3$): δ = 204.6, 88.5, 40.2, 34.5, 33.9, 32.2, 20.5, 20.3, 17.8, 17.3, 14.3 ppm; HRMS (ESI-QTOF) calcd for $C_{14}H_{28}NO_2^+$ [M + H^+]: 242.2100, found: 242.2102.

Primary Alcohol ***1a*** *((S)-2-((2,2,6,6-Tetramethylpiperidin-1-yl)-oxy)pentan-1-ol).* To a solution of α-oxyaldehyde **6** (96 mg, 0.4 mmol, 1.0 equiv) in 5 mL of ethanol was added sodium borohydride (101 mg, 3.6 mmol, 9.0 equiv). The reaction mixture was stirred for 5 min, then partitioned between ether (20 mL) and water (20 mL). The aqueous layer was extracted with ether (20 mL), and the combined organic layers were washed with brine (10 mL), dried over Na_2SO_4, and concentrated to give a colorless oil. Flash column chromatography (5% EtOAc/hexanes) gave primary alcohol **1a** (85 mg, 87%) as a colorless oil. **1a**: R_f = 0.27 (10% EtOAc/hexanes) $[\alpha]_D^{23} = -62.3°$ (*c* = 1.00, $CHCl_3$); IR (thin film): ν_{max} = 3576, 3018, 2925, 1465 cm^{-1}; ^{1}H NMR (600 MHz, $CDCl_3$): δ = 5.99 (s, 1H), 4.27 (s, 1H), 3.96 (dd, *J* = 11.9, 10.0 Hz, 1H), 3.57 (d, *J* = 9.5 Hz, 1H), 1.70−1.01 (m, 22H), 0.93 (t, *J* = 7.2 Hz, 3H) ppm; ^{13}C NMR (150 MHz, $CDCl_3$): δ = 68.8, 40.5, 39.8, 34.8, 33.5, 32.5, 20.6, 19.3, 17.3, 14.4 ppm; HRMS (ESI-QTOF) calcd for $C_{14}H_{30}NO_2^+$ [M + H^+]: 244.2300, found: 244.2271.

anti Diol ***3a*** *((3R,4S)-4-((2,2,6,6-Tetramethylpiperidin-1-yl)oxy)-hept-1-en-3-ol).* To a solution of aldehyde **6** (100 mg, 0.4 mmol, 1.0 equiv) in 400 μL of THF at −78 °C was added vinylmagnesium bromide (1.0 M in THF, 600 μL, 0.6 mmol, 1.5 equiv) dropwise over 3 min. The resultant solution was stirred at −78 °C for 30 min, then warmed to ambient temperature. The reaction mixture was partitioned between saturated NH_4Cl (5 mL) and ether (10 mL). The organic phase was washed with water (2 × 10 mL) and brine (10 mL), dried over Na_2SO_4, and concentrated to give a colorless oil. Flash column chromatography (5% EtOAc/hexanes) gave alcohol **3a** (77 mg, 71% yield) and a mixture of alcohol **3a** and the epimeric alcohol **2a** (7 mg, 6% yield) as colorless oils. **3a**: R_f = 0.42 (10% EtOAc/hexanes); $[\alpha]_D^{23} = -10.3°$ (*c* = 1.00, $CHCl_3$); IR (thin film): ν_{max} = 3450, 1642 cm^{-1}; ^{1}H NMR (600 MHz, $CDCl_3$): δ = 5.93 (ddd, *J* = 17.4, 10.5, 6.2 Hz, 1H), 5.28 (d, *J* = 17.3 Hz, 1H), 5.18 (d, *J* = 10.7 Hz, 1H), 4.44 (s, 1H), 3.98 (m, 1H), 2.49 (d, *J* = 3.6 Hz, 1H), 1.76 (m, 1H), 1.63−1.04 (m, 21 H), 0.90 (t, *J* = 7.3 Hz, 3H) ppm; ^{13}C NMR (150 MHz, $CDCl_3$): δ = 137.5, 115.9, 84.2, 73.9, 60.4, 40.8, 34.4, 31.1, 19.9, 17.3, 14.7, 14.3 ppm; $^3J_{H3-H4}$ = 4 Hz, $^2J_{H3-C4}$ = −3.1 Hz, $^2J_{H4-C3}$ = −1.0 Hz, $^3J_{H3-C5}$ = +1.2 Hz, $^3J_{H4-C2}$ = +3.1 Hz; HRMS (ESI-QTOF) calcd for $C_{16}H_{32}NO_2^+$ [M + H^+]: 270.2400, found: 270.2431.

syn Diol ***2a*** *((3S,4S)-4-((2,2,6,6-Tetramethylpiperidin-1-yl)oxy)-hept-1-en-3-ol).* To alcohol **3a** (1.56 g, 5.8 mmol, 1.0 equiv) in 12 mL of THF was added a solution of IBX (2.45 g, 8.7 mmol, 1.5 equiv) in 10 mL of DMSO. The reaction mixture was stirred for 1.5 h, then diluted with 20 mL of ether and filtered. The organic phase was washed with water (2 × 20 mL) and brine (20 mL), dried over Na_2SO_4, and concentrated to give an enone ((*S*)-4-((2,2,6,6-tetramethylpiperidin-1-yl)oxy)hept-1-en-3-one) (1.20 g, 79%) as a

DOI: 10.1021/acs.joc.5b01516
J. Org. Chem. 2015, 80, 9967−9972

colorless oil. The enone was used without purification in the next reaction.

To this enone (1.20 g, 4.5 mmol, 1.0 equiv) in 6 mL of THF and 18 mL of MeOH was added $CeCl_3 \cdot 7H_2O$ (3.36 g, 9.0 mmol, 2.0 equiv). The reaction mixture was stirred for 15 min, then cooled to −20 °C. $NaBH_4$ (513 mg, 13.6 mmol, 3.0 equiv) was added, and the resultant mixture was stirred for 2 h. The reaction mixture was partitioned between ether (50 mL) and water (100 mL). The aqueous layer was extracted with ether (100 mL), and the combined organic layers were washed with brine (50 mL), dried over Na_2SO_4, and concentrated to give a colorless oil. Flash column chromatography (5% EtOAc/hexanes) gave allylic alcohol **2a** (800 mg, 67%) and a mixture of alcohol **2a** and epimeric alcohol **3a** (110 mg, 9%) as colorless oils. **2a**: R_f = 0.36 (10% EtOAc/hexanes); $[\alpha]_D^{23}$ = −28.6° (c = 1.00, $CHCl_3$); IR (thin film): ν_{max} = 3438, 1641 cm^{-1}; ^1H NMR (600 MHz, $CDCl_3$): δ = 7.55 (br s, 1H), 5.74 (ddd, J = 17.1, 10.5, 6.8 Hz, 1H), 5.33 (d, J = 17.0 Hz, 1H), 5.14 (d, J = 10.4 Hz, 1H), 4.33 (t, J = 7.7 Hz, 1H), 3.87 (dt, J = 2.8, 8.7 Hz, 1H), 1.65−1.08 (m, 22H), 0.90 (t, J = 7.2 Hz, 3H) ppm; ^{13}C NMR (150 MHz, $CDCl_3$): 137.8, 116.8, 82.7, 78.1, 61.8, 60.3, 40.5, 40.0, 34.6, 33.6, 32.0, 20.73, 20.67, 18.9, 17.3, 14.5 ppm; HRMS (ESI-QTOF) calcd for $C_{16}H_{32}NO_2^+$ [M + H^+]: 270.2400, found: 270.2434.

■ ASSOCIATED CONTENT

Supporting Information

The Supporting Information is available free of charge on the ACS Publications website at DOI: 10.1021/acs.joc.5b01516.

^1H and ^{13}C NMR spectra, and calculated Cartesian coordinates and total energies (PDF)

■ AUTHOR INFORMATION

Corresponding Authors

*E-mail: twindus@iastate.edu (T.L.W.).
*E-mail: jschen@iastate.edu (J.S.C.).

Author Contributions

†These authors contributed equally.

Notes

The authors declare no competing financial interest.

■ ACKNOWLEDGMENTS

This research is supported by the National Science Foundation (T.L.W. and E.L.F.: OCI-1216566; J.S.C. and S.C.: CHE-1453896; NMR instrument: MRI-1040098). We thank Shu Xu (Iowa State University) for assistance with 2D NMR.

■ REFERENCES

(1) (a) Schröder, M. *Chem. Rev.* **1980**, *80*, 187. (b) Kolb, H. C.; VanNieuwenhze, M. S.; Sharpless, K. B. *Chem. Rev.* **1994**, *94*, 2483.

(2) (a) Rabjohn, N. *Org. React.* **1976**, *24*, 261. (b) Umbreit, M. A.; Sharpless, K. B. *J. Am. Chem. Soc.* **1977**, *99*, 5526.

(3) (a) Prein, M.; Adam, W. *Angew. Chem., Int. Ed. Engl.* **1996**, *35*, 477. (b) Stratakis, M.; Orfanopoulos, M. *Tetrahedron* **2000**, *56*, 1595.

(4) Davis, F. A.; Chen, B. C. *Chem. Rev.* **1992**, *92*, 919.

(5) (a) Sibi, M. P.; Hasegawa, M. *J. Am. Chem. Soc.* **2007**, *129*, 4124. (b) Pouliot, M.; Renaud, P.; Schenk, K.; Studer, A.; Vogler, T. *Angew. Chem., Int. Ed.* **2009**, *48*, 6037. (c) Kano, T.; Mii, H.; Maruoka, K. *Angew. Chem., Int. Ed.* **2010**, *49*, 6638. (d) Van Humbeck, J. F.; Simonovich, S.; Knowles, R. R.; MacMillan, D. W. C. *J. Am. Chem. Soc.* **2010**, *132*, 10012. (e) Simonovich, S. P.; Van Humbeck, J. F.; MacMillan, D. W. C. *Chem. Sci.* **2012**, *3*, 58. (f) Dinca, E.; Hartmann, P.; Smrček, J.; Dix, I.; Jones, P. G.; Jahn, U. *Eur. J. Org. Chem.* **2012**, *2012*, 4461. (g) Xie, Y.-X.; Song, R.-J.; Liu, Y.; Liu, Y.-Y.; Xiang, J.-N.; Li, J.-H. *Adv. Synth. Catal.* **2013**, *355*, 3387. (h) Ho, X.-H.; Jung, W.-J.; Shyam, P. K.; Jang, H.-Y. *Catal. Sci. Technol.* **2014**, *4*, 1914.

(6) (a) Liu, H.; Feng, W.; Kee, C. W.; Zhao, Y.; Leow, D.; Pan, Y.; Tan, C.-H. *Green Chem.* **2010**, *12*, 953. (b) Koike, T.; Yasu, Y.; Akita, M. *Chem. Lett.* **2012**, *41*, 999. (c) Luo, X.; Wang, Z.-L.; Jin, J.-H.; An, X.-L.; Shen, Z.; Deng, W.-P. *Tetrahedron* **2014**, *70*, 8226.

(7) (a) Fuller, P. H.; Kim, J.-W.; Chemler, S. R. *J. Am. Chem. Soc.* **2008**, *130*, 17638. (b) Karyakarte, S. D.; Smith, T. P.; Chemler, S. R. *J. Org. Chem.* **2012**, *77*, 7755. (c) Sanjaya, S.; Chua, S. H.; Chiba, S. *Synlett* **2012**, *23*, 1657. (d) Han, B.; Yang, X.-L.; Fang, R.; Yu, W.; Wang, C.; Duan, X.-Y.; Liu, S. *Angew. Chem., Int. Ed.* **2012**, *51*, 8816. (e) Hartmann, M.; Li, Y.; Studer, A. *J. Am. Chem. Soc.* **2012**, *134*, 16516. (f) Zhang, B.; Studer, A. *Org. Lett.* **2013**, *15*, 4548. (g) Dutta, U.; Maity, S.; Kancherla, R.; Maiti, D. *Org. Lett.* **2014**, *16*, 6302.

(8) (a) Yoon, H.-S.; Ho, X.-H.; Jang, J.; Lee, H.-J.; Kim, S.-J.; Jang, H.-Y. *Org. Lett.* **2012**, *14*, 3272. (b) Li, Y.; Vogler, T.; Renaud, P.; Studer, A.; Pouliot, M. *Org. Lett.* **2012**, *14*, 4474. (c) Shyam, P. K.; Jang, H.-Y. *Eur. J. Org. Chem.* **2014**, *2014*, 1817.

(9) Abeykoon, G. A.; Chatterjee, S.; Chen, J. S. *Org. Lett.* **2014**, *16*, 3248.

(10) Matsumori, M.; Kaneno, D.; Murata, M.; Nakamura, H.; Tachibana, K. *J. Org. Chem.* **1999**, *64*, 866.

(11) Allen, M. J.; Keal, T. W.; Tozer, D. J. *Chem. Phys. Lett.* **2003**, *380*, 70.

(12) Stephens, P. J.; Devlin, F. J.; Chabalowski, C. F.; Frisch, M. *J. Phys. Chem.* **1994**, *98*, 11623.

(13) Schmidt, M. W.; Baldridge, K. K.; Boatz, J. A.; Elbert, S. T.; Gordon, M. S.; Jensen, J. H.; Koseki, S.; Matsunaga, N.; Nguyen, K. A.; Su, S. J.; Windus, T. L.; Dupuis, M.; Montgomery, J. A. *J. Comput. Chem.* **1993**, *14*, 1347.

(14) Binkley, J. S.; Pople, J. A.; Hehre, W. J. *J. Am. Chem. Soc.* **1980**, *102*, 939.

(15) Head-Gordon, M.; Pople, J. A.; Frisch, M. J. *Chem. Phys. Lett.* **1988**, *153*, 503.

(16) Frisch, M. J.; Pople, J. A.; Binkley, J. S. *J. Chem. Phys.* **1984**, *80*, 3265.

(17) Pettersen, E. F.; Goddard, T. D.; Huang, C. C.; Couch, G. S.; Greenblatt, D. M.; Meng, E. C.; Ferrin, T. E. *J. Comput. Chem.* **2004**, *25*, 1605.

(18) Valiev, M.; Bylaska, E. J.; Govind, N.; Kowalski, K.; Straatsma, T. P.; Van Dam, H. J. J.; Wang, D.; Nieplocha, J.; Apra, E.; Windus, T. L.; De Jong, W. A. *Comput. Phys. Commun.* **2010**, *181*, 1477.

(19) Wolinski, K.; Hinton, J. F.; Pulay, P. *J. Am. Chem. Soc.* **1990**, *112*, 8251.

(20) Kendall, R. A.; Dunning, T. H., Jr.; Harrison, R. J. *J. Chem. Phys.* **1992**, *96*, 6796.

DOI: 10.1021/acs.joc.5b01516
J. Org. Chem. 2015, 80, 9967−9972